Design and Validation of a 3-DoF Wrist Perturbator Based on an Inverted Spatial Redundant 4-RUU Parallel Manipulator

Koene, Robbert; Meijaard, Jaap; van de Ruit, Mark; Mugge, Winfred; van der Wijk, Volkert

DOI
10.1007/978-3-031-45705-0_76

Publication date
2023

Document Version
Final published version

Published in
Advances in Mechanism and Machine Science

Citation (APA)
Koene, R., Meijaard, J., van de Ruit, M., Mugge, W., & van der Wijk, V. (2023). Design and Validation of a 3-DoF Wrist Perturbator Based on an Inverted Spatial Redundant 4-RUU Parallel Manipulator. In M. Okada (Ed.), *Advances in Mechanism and Machine Science : Proceedings of the 16th IFToMM World Congress 2023* (Vol. 1, pp. 786-796). (Mechanisms and Machine Science; Vol. 147). Springer. https://doi.org/10.1007/978-3-031-45705-0_76

Design and Validation of a 3-DoF Wrist Perturbator Based on an Inverted Spatial Redundant 4-RUU Parallel Manipulator

Robbert Koene[1], Jaap Meijaard[1], Mark van de Ruit[2], Winfred Mugge[2], and Volkert van der Wijk[1(✉)]

[1] Department of Precision and Microsystems Engineering, Delft, Netherlands
V.vanderWijk@tudelft.nl

[2] Department of BioMechanical Engineering of Delft University of Technology, Delft, Netherlands

Abstract. Humans vary the stiffness in their joints depending on tasks and circumstances. For posture control a high joint stiffness is required to withstand perturbations, whereas for force control a low joint stiffness is required. To investigate how humans vary their joint stiffness precisely for moving an arm, a wearable device is needed that can generate small force perturbations at the wrist while measuring the resulting muscular reactions. The majority of the state-of-the-art devices either offer too little versatility or impede the free movement of the arm. Based on a 3-DoF spatial redundant 4-RUU parallel manipulator applied in an inverted way where the original base with actuators has become the moving platform and the original moving platform is attached to the wrist as a bracelet, a versatile, 0.175 kg lightweight, low impedance, and compact wearable device was developed that can generate perturbation forces in X-, Y-, and Z-direction. The design and a prototype of the device are presented with experimental tests showing controlled perturbations in the order of 4 N with frequencies up to 12 Hz.

Keywords: Force perturbation · Wearable device · Human arm · System identification · Bracelet · Parallel manipulator · Mechatronics

1 Introduction

System identification has been used for decades to determine the mechanical properties of the human limbs [1]. Originally, these experiments entailed robotic manipulators applying perturbations to a human joint in a laboratory setting. Due to scientific developments in the field of robotics [2] and healthcare [3], measurements outside the laboratory in the normal human environment are needed. By using wearable measurement devices it is possible to do experiments during daily tasks without impeding voluntary movements.

For arm perturbators a multitude of wearable devices exist, differing mainly in their actuation principle and resulting specifications. With pneumatics it is

M. Okada (Ed.): IFToMM WC 2023, MMS 147, pp. 786–796, 2023.
https://doi.org/10.1007/978-3-031-45705-0_76

possible to generate well-defined and versatile perturbation forces. By implementing the airjet principle [4], a perturbation force of 4 N with a frequency of 75 Hz is achievable. A solution with perturbation forces in three different directions is realized by mounting a block with multiple outlets on the wrist [5]. The working principle behind these designs is the venting of pressurized air into the atmosphere, generating also considerable noise. Using the air pressure to move a mass instead of venting for generating a perturbation force results in a quieter device [6]. Still, the major drawback of all pneumatics based systems is the bulky peripheral equipment such as pressure tank, tubes, and valves that is needed.

Electro-mechanical solutions exist in the form of rotating and translating assemblies. Rotating assemblies can generate force or torque perturbations by using flywheel inertia [7] or the gyroscopic effect [8]. However, as a side effect the gyroscopic stabilization of rotating bodies impedes voluntary movement. Current translational solutions consist of crank [9] and cam [10] mechanisms that are able to produce repeatable force perturbations with high amplitudes. Unfortunately, these 1-DoF mechanisms also generate substantial parasitic forces.

The majority of current electro-mechanical solutions have been designed to be applied to the arm, however little effort has been made to lower or eliminate their impedance. Some devices are placed on the wrist off-axis, inducing torques as well. Other solutions consist of significant rectangular or cylindrical objects and are required to be hand-held. In addition, most existing actuation principles generate perturbation forces in solely a single direction and need to be stacked for multi-directional force perturbations, resulting in inefficient and bulky devices.

The goal of this paper is to present a proof-of-concept mechatronic device designed to be compact, lightweight, and wearable and to generate controlled force perturbations in X-, Y-, and Z-direction at the wrist. This is achieved by using high performance servo motors together with a novel inverted implementation of a spatial redundant three-degrees-of-freedom (3-DoF) 4-RUU parallel manipulator. Since the device is intended for non-intrusive system identification, design choices have been made with this purpose in mind. First the parallel mechanism and its kinematics are explained and subsequently the prototype device is presented and described in detail. Then an experimental evaluation of the performance of the prototype is shown and points for improvement are discussed.

2 Design

The working principle of the design is based on Newton's second and third law of motion, where the acceleration of a mass results in a reaction force proportional and opposite to this acceleration. This relation enables a lightweight design to generate a suitably large perturbation force, as long as the mechanism can provide ample acceleration.

2.1 The Mechanism

To generate perturbation forces in the three directions X, Y, and Z by moving a mass, a device with three translational DoFs is needed. Different from stacking

three 1-DoF mechanisms in series, implementing a 3-DoF parallel mechanism leads to a significantly less bulky and an efficient design. In addition, parallel mechanisms offer a high stiffness and are known for their excellent dynamic behaviour [11]. For this particular application the Delta manipulator [12] is a suitable starting point.

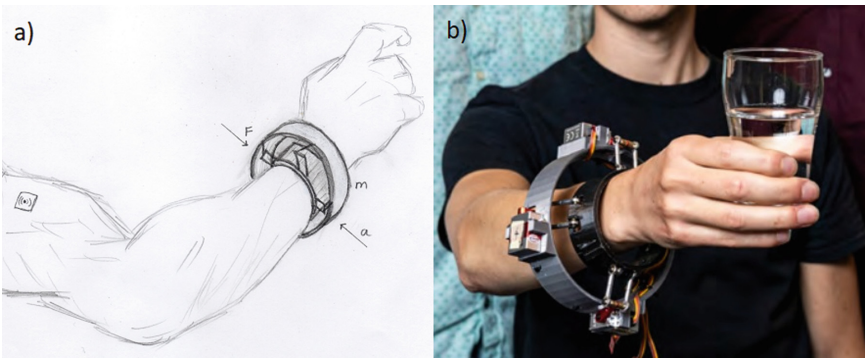

Fig. 1. (a) Concept of a device with parallel mechanism connecting an inner ring attached to the wrist with an outer motion controlled ring enabling free movement of the arm while doing measurements on the arm; (b) The developed prototype device mounted on a person's wrist

Due to its typical geometry, a parallel manipulator mechanism is perfectly suitable for construction around the wrist, necessary to avoid axial rotational perturbations and leaving the person's hands free for doing tasks. Therefore, the base of the mechanism was chosen to be a ring, tightly fitted around the wrist as illustrated in Fig. 1a. The large moving element of the mechanism, in robotics called the end-effector or moving platform, is also chosen to be a ring around the wrist but with a larger diameter than the base such that it has space to move towards and away from the arm. The two rings are connected with kinematic chains—i.e. robotic legs—such that the outer ring is constrained to move solely with 3-DoF translational motions. For this, three RUU legs as in the Delta manipulator are sufficient, where R represents a revolute joint and U a universal joint.

Since the large outer ring needs to have significant mass for generating the perturbation forces, contrary to conventional designs of parallel manipulators that have the actuators at the base, here it is chosen to place the actuators on the moving platform, i.e. on the outer ring. The mass of the actuators then is effectively used to generate perturbation forces with the total mass of the device remaining relatively low. Such a design can be regarded an inverted application of a parallel manipulator where the original base with actuators has become the moving platform and the original moving platform has become the base of the robot. The inverted application means that each leg has a revolute joint with the

moving platform which is driven by an actuator and that the leg elements connected to the base ring around the wrist consist of the well-known parallelograms of the Delta manipulator with universal joints on each side.

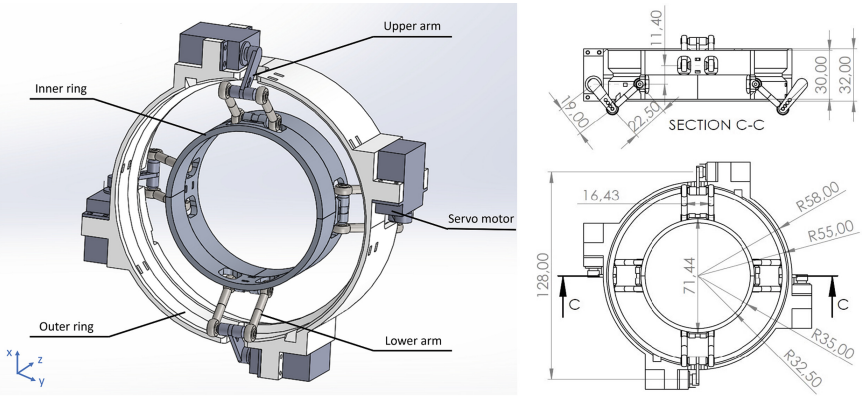

Fig. 2. CAD model of the prototype with the main dimensions (in mm). The Z-axis is defined in the longitudinal direction with the X- and Y-axis in the transverse plane

2.2 Redundant Leg and CAD

In order to obtain a compact device and to avoid axial rotational perturbations it is preferred to have the outer ring and inner ring be concentric and coplanar when in home position. With the Delta manipulator mechanism this is not possible since this pose is a singularity. Therefore it was chosen to add a fourth driven leg equal to the three legs to obtain both kinematic redundancy as well as actuation redundancy and to distribute the four legs equally around the wrist with one pair of opposite motors acting from one side and the other pair of opposite motors acting from the other side mounted on the rings with an out-of-plane offset between both pairs of motors. Figure 2 shows the CAD model of this new manipulator with the dimensions where the lengths of the links of the legs were determined by a close to 90° angle between both links when in the home pose for which the sensibility to the singularities was found to be the lowest. The outer ring is able to move at least 8 mm from its home position in all directions relative to the inner ring, allowing maximal displacements of 16 mm.

General other advantages of redundancy are known as that play in the joints is reduced or eleminated and the mechanism stiffness is increased [11], and that its performance is boosted [13,14].

Since for the production of the prototype it was chosen to select as much as possible off-the-shelf components, the device was designed with micro ball joints instead of universal joints as shown in Fig. 2. This means that all the links connected to the inner ring are underconstrained and can freely rotate

about their longitudinal axis. Since this rotational motion is limited by physical boundaries and does not affect the motion of the outer ring, this has no influence on the functioning of the device.

3 Prototype

3.1 Production

The developed prototype of the wrist perturbator is shown in Fig. 1b and in Fig. 3a. Both the inner and the outer ring have been manufactured of PLA polymer by 3D printing. The inner ring was produced to be dividable in two halves (not shown in Fig. 2) for mounting it tightly around the wrist by screwing the halves together. Using a material stiffer than PLA would be beneficial for the stiffness of the device, however 3D printing with PLA is sufficient for the proof-of-concept and practical for including all the attachment points and details. The moving mass of the device, i.e. the mass of the outer ring including the actuators, is 0.146 kg and the total mass of the complete device as shown is with 0.175 kg significantly lightweight.

3.2 Actuation

For the actuation of the prototype the KST DS215MG V3.0 servo motor was selected. In addition to excellent performance characteristics as shown in Table 1, the implementation of this motor is very practical since it consists of a gearbox, an encoder, and an internal controller in one. With two ball bearings the motor is strong and robust. It has a small footprint and low weight while generating significantly high torques at relatively high speeds. The motor operates at 7.4 V, which is the rated voltage of compact two cell LiPo battery packs and a safe voltage to use for human contact.

Table 1. Specifications of the KST DS215MG V3.0 servo motor

Operating voltage (V)	6.0 or 7.4
Torque (Nm)	0.30 or 0.36
Angular velocity (rad/s)	34.9 or 41.9
Control frequency (Hz)	333
Dimensions ($l \times w \times h$) (mm^3)	$23 \times 12 \times 27.5$
Weight (g)	20

The control of the motors is also rather simple, for which an Arduino Nano was used. The Arduino communicates via a pulse width modulated (PWM) signal sending the desired motor angles at each time step for position control. The internal motor controller then rotates the motor axle to the desired angle

with an internal feedback loop of which no (encoder) data is accessible. Also the control parameters are not tunable. It is remarkable that with this equipement also the complete system of the device, the Arduino Nano controller, and a two cell LiPo battery pack is very compact, fully wearable, and lightweight.

For redundantly controlled manipulators generally it is important in the control to distribute the actuator torques well among the actuators for best performance and to omit the generation of internal forces which can become significantly high [14]. With these motors that is not possible. Since the maximal motor torques are too low to break the device, this however is not a risk here although the performance and power consumption may not be optimal.

3.3 Motion Control

The motion of the outer ring can be programmed such that the device generates either a transient or a periodic pulse or force perturbation. For the aimed purpose of system identification a suitable choice of acceleration profile is a block wave representing a step function. The control algorithm has as inputs the desired displacement and direction of the perturbation force, for instance from -0.005 to 0.005 m along the X-axis, and the (max) acceleration derived from the desired perturbation force from which the pulse length and the position of the outer ring at each time step are calculated. With the inverse kinematic model [12] this trajectory of positions is turned into an array of the corresponding motor angles at each time step which then is converted into the input signals for each motor.

The derived motor angles were also used as input for simulations of the device in Simscape, with which the performance could be validated by the generated reaction forces and reaction moments on the base i.e. wrist and insight in the motor torques and motor velocities could be obtained.

4 Experimental Measurements

4.1 Experimental Set-Up

The prototype was experimentally tested in the setup shown in Fig. 3. The inner ring was mounted on a 3D printed artificial wrist which was mounted on an ATI mini45 6-DoF force-torque sensor to measure the generated perturbation forces. The sensor was placed perfectly horizontally such that also the transversal plane or XY-plane of the prototype was perfectly horizontal with the Z-axis pointing upwards. The output of the sensor was sampled at 10 kHz, passed through a 5 V amplifier and was then processed by a NI USB-6361 DAQ. By a USB connection, the six signals were led into a MATLAB script where the signals were multiplied with the sensor's calibration matrix resulting into the measured force and torque values. Each measurement began with powering on the prototype in its home position. The first measured values of each measurement were averaged and subtracted from the complete measurement to correct for offset and for the influence of gravity.

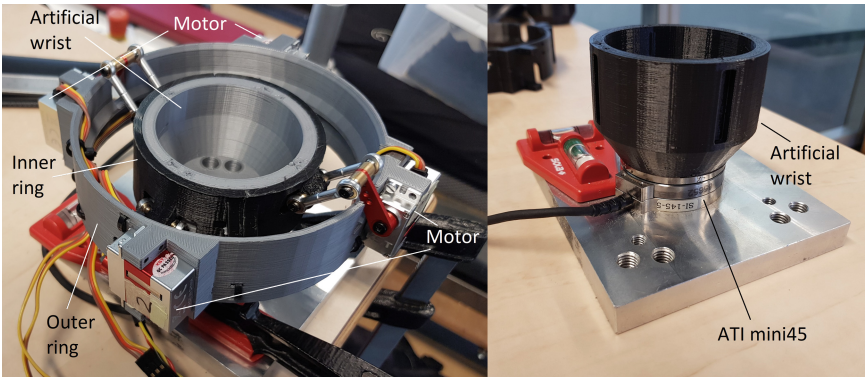

Fig. 3. The wrist perturbator prototype mounted on an artificial wrist that is mounted on an ATI Mini45 6-DoF force-torque sensor for measurement of the generated perturbation forces

4.2 Experiments

As a preparation for the final performance experiment, some initial tests were performed to check the control and overall functioning of the system. It was empirically determined that the motors' maximum rotational velocity was 32 rad/s, when loaded. This value was used for the motion planning. During the first experiments it became clear that this rotational velocity was severely limiting the capabilities of the device. For large displacements and high accelerations the motors quickly reached their top speed. High perturbation forces of 8 N were still achievable, but this required an acceleration profile different from a block wave or the increase of the weight of the outer ring for which accelerations can be lower. The choice for a block wave acceleration profile therefore does not give the highest possible force perturbations with this device.

The following tests were performed: a 3 N periodic and 4 N transient force perturbation for 10 mm displacements about the home position in X-, Y-, and Z-direction. Since during daily tasks the direction of the gravity force changes continuously as the arm moves around, the prototype was tested both horizontally as in Fig. 3 and vertically being 90° rotated about the Y-axis.

4.3 Results

Figure 4 shows the results of the periodic tests, together with the theoretical values. The average measured force is displayed with a solid line and the standard deviation is represented by dotted lines. The plots represent one full cycle of the mechanism and while a periodic signal can be detected, it does not entirely resemble the desired block wave. The zero-crossing occurs halfway the trajectory, when the outer ring changes from acceleration to deceleration. A quarter period to both sides from this point there is a dip. This is most likely due to the motors having to switch directions. The other dips in the values are attributed to the

internal controller of the servos which process the angular inputs at 333 Hz (every 3 ms) which turns out too slow for this motion. This was proved by increasing the moving mass for which the acceleration to generate an equal force perturbation is lower and more data points are available for the controller, showing indeed a smoother output. Comparing the two orientations of the prototype shows that there is no change in the generated force perturbation and that gravity has no influence on the performance.

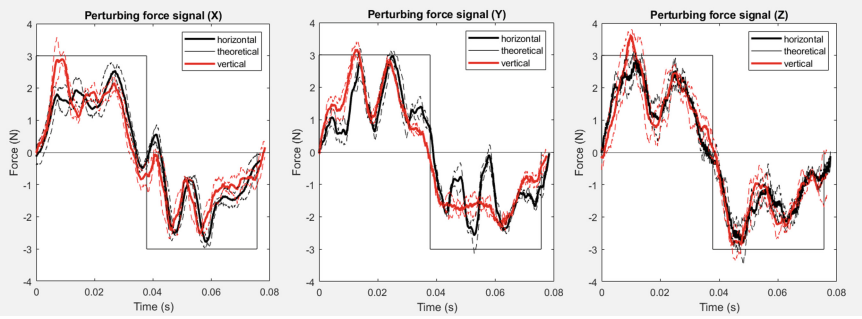

Fig. 4. 3 N force perturbations in X, Y, and Z direction with the gravity force in the Z-direction in black and when set-up is rotated 90° around the Y-axis with the gravity force in the X-direction in red

Figure 5 shows the measured forces for a one-way motion in X-, Y-, and Z-direction. Also here the average measured force is displayed with a solid line and the standard deviation is represented by dotted lines. The value of 4 N is reached during deceleration as a peak. The signal is smoother during acceleration, but then does not reach the 4 N. This could be a result of the backlash in the joints, or the unfavourable position of the arms at the edges of the workspace. Combined with the non-optimal controller, this can result in undershoot or overshoot.

During the experiments also the parasitic forces and moments were measured. Although not displayed here, generally their values were significantly low. Parasitic forces tended to become larger when reaching the outer limits of the workspace in the transversal XY-plane.

5 Discussion

The force perturbations that can be generated by the prototype are a trade-off among different parameters. The force magnitude depends on the weight of the moving mass and its acceleration while the acceleration together with the size of the stroke influence the length of the perturbation and the maximum bandwidth. Therefore the user has to determine which shape and size of the perturbation is desired for which all combinations have not yet been evaluated.

Some rough specifications of the presented design can be derived from observing the prototype and by inspecting the experimental data. The maximum travel

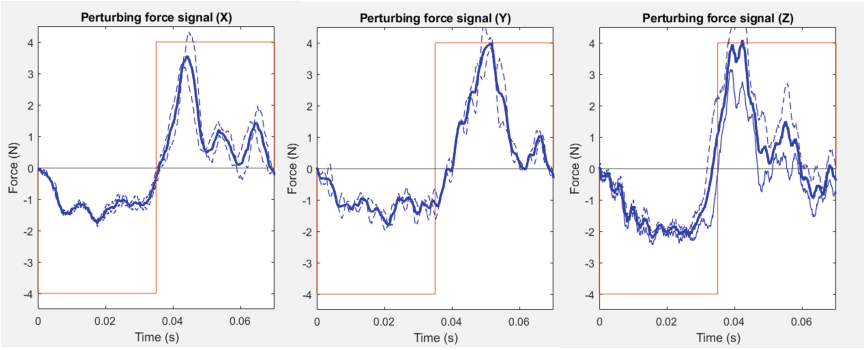

Fig. 5. 4 N transient force perturbations in X-, Y-, and Z-direction

was measured to be 16 mm in all directions. The nominal force perturbation for square wave acceleration profiles is limited to roughly 4 N at a maximum bandwidth of 12 Hz. These outcomes showed to be repeatable with an average standard deviation of 0.20 N, 0.22 N, and 0.53 N in X-, Y-, and Z-direction, respectively. A maximum force perturbation of about 8 N for a high-frequency peak acceleration was shown possible.

The fourth redundant leg increased the mechanism's stiffness, while decreasing its sensitivity to singular positions. Yet, due to significant play in the ball joints the stiffness decreased when moving away from the home position. Also some hysteresis can be observed in the results of the periodic experiments. It is recommended to implement precise play-free universal joints, to design stiffer rings, and to optimize the geometry to improve the performance of the design.

The chosen actuators showed excellent simplicity for implementation and control. However its internal controller gave poor setpoint tracking, especially due to the redundancy of the mechanism, limiting the performance significantly. Since it is known that redundant parallel manipulators benefit from customized control [15] this would lead to a significant improvement. Also the motors' gear ratio should be optimized and reduced to increase its maximum angular velocity needed for generating higher perturbation forces.

6 Conclusion

In this paper, a proof-of-concept wearable mechatronic device was presented that is able to generate controlled transient or up to 12 Hz periodic force perturbations of 4 N in X-, Y-, and Z-direction at the wrist for measurements on the human arm. With respect to the state of the art, this device has a high level of versatility, is compact and lightweight with just 0.175 kg, and has a significantly low impedance to voluntary movements.

The design of the device is based on a novel inverted implementation of a redundant three-degrees-of-freedom spatial 4-RUU parallel manipulator to keep the design as compact as possible and for minimal parasitic torques. Small powerful servo motors were selected to redundantly actuate the mechanism for high

performance and simple implementation of the control electronics. By experiments the viability and potential of the device was shown. Since the automatic internal controller of the servo motors showed to be limiting, the performance of the device can be improved by implementing motors with dedicated motor control.

References

1. Kearney, R., Hunter, I.: System identification of human joint dynamics. Crit. Rev. Biomed. Eng. **18**, 55–87 (1990)
2. Angelini, F., Della Santina, C., Garabini, M., Bianchi, M., Bicchi, A.: Control architecture for human-like motion with applications to articulated soft robots. Front. Robot. AI **7** (2020). https://doi.org/10.3389/frobt.2020.00117
3. Piggott, L., Wagner, S., Ziat, M.: Haptic neurorehabilitation and virtual reality for upper limb paralysis: a review. Crit. Rev. Biomed. Eng. **44**, 1–32 (2016). https://doi.org/10.1615/CritRevBiomedEng.2016016046
4. Xu, Y., Hunter, I.W., Hollerbach, J.M., Bennett, D.J.: An airjet actuator system for identification of the human arm joint mechanical properties. IEEE Trans. Biomed. Eng. **38**, 1111–1122 (1991)
5. Gurocak, H., Jayaram, S., Parrish, B., Jayaram, U.: Weight sensation in virtual environments using a haptic device with air jets. ASME J. Comput. Inf. Sci. Eng. **3**, 130–135 (2003). https://doi.org/10.1115/1.1576808
6. Höppner, H., Lakatos, D., Urbanek, H., van der Smagt, P.: The arm-perturbator: design of a wearable perturbation device to measure limb impedance. In: Proceedings, First International Conference on Applied Bionics and Biomechanics, ICABB-2010. Venice, Italy, October 14–16 (2010)
7. Walker, J.M., Raitor, M., Mallery, A., Culbertson, H., Stolka, P., Okamura, A.M.: A dual-flywheel ungrounded haptic feedback system provides single-axis moment pulses for clear direction signals. In: 2016 IEEE Haptics Symposium (HAPTICS), pp. 7–13 (2016). https://doi.org/10.1109/HAPTICS.2016.7463148
8. Hondori, H.M., Ang, W.T.: Smart mug to measure hand's geometrical mechanical impedance. In: Proceedings 33rd Annual International Conference of the IEEE Engineering in Medicine and Biology Society, pp. 4053–4056 (2011). https://doi.org/10.1109/IEMBS.2011.6091007
9. Amemiya, T., Kawabuchi, I., Ando, H., Maeda, T.: Double-layer slider-crank mechanism to generate pulling or pushing sensation without an external ground. In: 2007 IEEE/RSJ International Conference on Intelligent Robots and Systems, pp. 2101–2106 (2007). https://doi.org/10.1109/IROS.2007.4399211
10. Kakuda, E., Yokota, S., Matsumoto, A., Chugo, D., Hashimoto, H.: Concept verification of ungrounded force display using cam. In: 2018 11th International Conference on Human System Interaction (HSI), pp. 432–437 (2018). https://doi.org/10.1109/HSI.2018.8431319
11. Patel, Y., George, P.: Parallel manipulators applications—a survey. Mod. Mech. Eng. **2**, 57–64 (2012). https://doi.org/10.4236/mme.2012.23008
12. Clavel, R.: Conception d'un robot parallèle rapide à 4 degrés de liberté. Ph.D. thesis, Département de Microtechnique, EPFL, Lausanne (1991)
13. Corbel, D., Gouttefarde, M., Company, O., Pierrot, F.: Towards 100G with PKM: is actuation redundancy a good solution for pick-and-place? In: 2010 IEEE International Conference on Robotics and Automation, pp. 4675–4682 (2010). https://doi.org/10.1109/ROBOT.2010.5509921

14. Van der Wijk, V., Krut, S., Pierrot, F., Herder, J.L.: Design and experimental evaluation of a dynamically balanced redundant planar 4-RRR parallel manipulator. I. J. Robot. Res. **32**(6), 744–759 (2013)
15. Nokleby, S., Fisher, R., Podhorodeski, R., Firmani, F.: Force capabilities of redundantly-actuated parallel manipulators. Mech. Mach. Theory **40**(5), 578–599 (2005). https://doi.org/10.1016/j.mechmachtheory.2004.10.005